

Original Research Paper

## Optimizing the diameter and curvature radius of a seed tube in pressurized pneumatic planting machines

Hosein Nasiri-Talashi, Abbas Rezaeiasl\*, Mohammad Hashem Rahmati

Department of Bio-system Mechanical Engineering, Gorgan University of Agricultural Sciences and Natural Resources, Gorgan, Iran

Biosystems Engineering and Renewable Energies 2025, 1 (1): 37-43

### KEYWORDS

response surface methodology  
image processing  
cylinder distributor  
uniform distribution  
partial least squares

### \* Corresponding author

abrezaeiasl@gmail.com  
arezaeiasl@gau.ac.ir

### Article history

Received: 2024-11-12

Revised: 2024-12-30

Accepted: 2025-01-10

### ABSTRACT

This study aimed to determine the effects of the diameter and curvature shape of a planter's seed tube on the uniformity of seed distribution and deviation from the cultivation line. The effects of tube diameter (at four levels, 5, 7, 9, and 11 mm) and tube curvature radius (at three levels, 5, 15, and 20 cm) were investigated on the quality of the seed distribution. The location of the seeds distributed by the planter was obtained by image processing techniques. The results revealed that the diameter and curvature radius of the seed tube did not have significant effects on the uniform distribution of seeds in the travel direction. However, the effects of both factors and their interaction were significant ( $P < 0.01$ ) on the deviation of seed locations from the cultivation row. Response surface methodology (RSM) was then utilized to optimize the average distance of the seeds in travel and its perpendicular directions. According to the results, the distance of the planted seeds can be optimized with high desirability rates ( $\approx 1$ ) based on the design parameters of pressurized pneumatic planters. Finally, the results showed that the partial least squares (PLS) method could efficiently predict the average distance of the seeds having the diameter and curvature radius of the seed tube with an  $R^2$  value equal to 0.99.

## 1. Introduction

Planters are one of the most important implements of seed cultivation. Since a large part of them are mechanical, their seed selection system (distributor) causes remarkable damage to the seeds leading to the reduction of seed germination percentage (Garg et al., 2019). Therefore, airflow-assisted pneumatic systems have been widely investigated in recent years. The effects of airflow velocity and rotation of pressurized metering drum have been studied on the uniformity of seed distribution. The results show that increasing the seed drum velocity reduces the uniformity coefficient of the seed distribution (Soares et al., 2020). Using a maize-soybean interplanting seeder, An et al. (2017) showed that the rotational speed of the distributor affected its measurement (counting) performance at different operating speeds of the planter. In another study, Cay et al. (2018a) introduced an electronic machine controller for a typical planter unit and evaluated its performance with a conventional controller system at different speeds and seed spacing in the laboratory. In another study, they investigated the effects of the developed control system on planting uniformity, planting space, fuel consumption, and slippage. The uniformity of planting distances was better using the introduced control system compared to a conventional control system (Cay et al., 2018b).

With the development of robust and efficient digital image processing techniques, images have become one of the essential sources of data and information in modern agricultural systems (Dubey et al., 2015). Image processing has been widely used in weed detection (Tang et al., 2016; Wang et al., 2019), plant health monitoring (Zhang et al., 2019), plant row detection (Zhai et al., 2016), robotic fruit harvesting (Barth et al., 2019), farmer-assistant systems (Asefpour Vakilian and Massah, 2017), and

food processing (Meruliya et al., 2015; Fellegari and Navid, 2011). Using image segmentation, object detection, and morphological operators, image processing programs, such as ImageJ and OpenCV, are extensively used in agricultural research to assess the quality of agricultural systems that can be difficult for the human eye. The location of seeds distributed by planters in field and laboratory setups can be easily tracked by image processing programs.

Several methods have been developed to find optimal values of model inputs in optimization problems to obtain a minimum or maximum value for the output. Although nature-inspired methods have been recently introduced to solve many optimization problems in science and engineering (Ma et al., 2019), some aged algorithms, such as response surface methodology (RSM), are still widely used by researchers for a wide range of problems (Sarlaki et al., 2020). RSM can lower the number of experiments required to find the behavior of the system, which can be time- and cost-effective. This method provides efficient graphical plots to investigate the optimal operating conditions through experimental methods. Generally, RSM includes several stages, i.e., data coding, creating the design, fitting the response surface model, and graphical representation of the response surface (Scheidt et al., 2020).

Due to the importance of planting distance and uniformity in the quality of seeders and planters' seed distributors, which can significantly affect the cultivation process, this study aims to: (a) determine the effects of the diameter and curvature radius of seed tube on the uniformity of seed distribution and deviation from the cultivation line, (b) optimize the average distance of the seeds in travel and its perpendicular directions using RSM, and (c) use the partial least squares (PLS) to predict the seeds' distance having the values of the planter parameters.

## 2. Materials and Methods

### 2.1. Seed distributor

This study was conducted using a pressurized seed metering drum constructed in the Department of Bio-system Mechanical Engineering at Gorgan University of Agricultural Sciences and Natural Resources, Gorgan, Iran. This system carries the rapeseed with the least possible damage from the seed tank to the flute on the cultivation row. In this system, the airflow generated by a blower causes a pressure difference inside and outside the metering drum. The pressure difference applies to the pressure force on the seed and attaches it to the back of the hole. As the drum rotates, the seed stuck to the back of the hole rotates with the drum and is located at the top of the seed tube. A strong airflow from the seed remover eliminates the air pressure difference, and the seed is removed from the back of the hole. It then enters the seed tube due to its weight and the flow of air passing through the tube, and it is carried to the end of the seed tube because of the airflow.

The shape of the seed tube diameter and its curvature radius can be effective in the uniform seed distribution. The effects of

tube diameter (at four levels, 5, 7, 9, and 11 mm) and tube curvature radius (at three levels, 5, 15, and 20 cm) were investigated on the quality of the seed distribution. Based on the tube curvature radius, three shapes of seed tubes were investigated in this study, namely, a, b, and c. The schematics of the planter and its parameters, i.e., the diameter and curvature radius of the seed tube, are depicted in Figure 1. All three seed tubes exited the metering drum with a curvature radius of 20 cm. In the first shape (a), the seeds arrived at the falling location with a curvature radius of 20 cm ( $r_1$ ). In the second shape (b), the seed tube became perpendicular downward after the first curvature, and the seeds then moved through two 15 cm curvatures ( $r_2$ ). The third shape (c) was similar to the second shape; however, instead of two 15 cm curvatures, two curvatures with radiuses of 5 cm ( $r_3$ ) were considered in its design. The smaller the curvature radius, the longer the seed tube is. Therefore, the length of the seed tubes was in the order of  $a < b < c$ . The constructed system with the seed tube is shown in Figure 2. A grease belt was used in this study for the accurate investigation of seed distribution after leaving the seed tube.

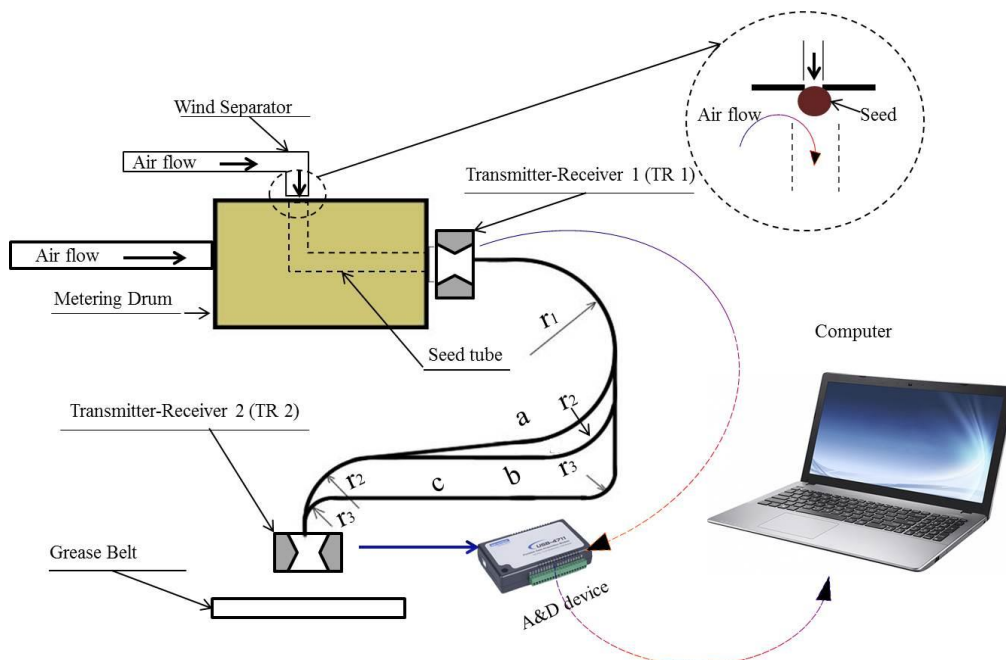


**Figure 1.** Schematics of a laboratory pneumatic planter and its parameters, i.e., diameter and curvature radius of the seed tube



**Figure 2.** The seed tube and grease belt constructed for the experiments. A light-sensitive displacement sensor was installed at the beginning of the tube, while another sensor was installed at the end of the tube to investigate the movement of the seeds in the tube. The sensors' data were transferred to a computer using an A/D converter for further analysis. An example of the output of the transmitter-receivers used in the seed tubes with different curvature radiuses is depicted in Figure 3. As shown in the figure, the movement of the seeds in the seed tube is affected by its curvature shape.

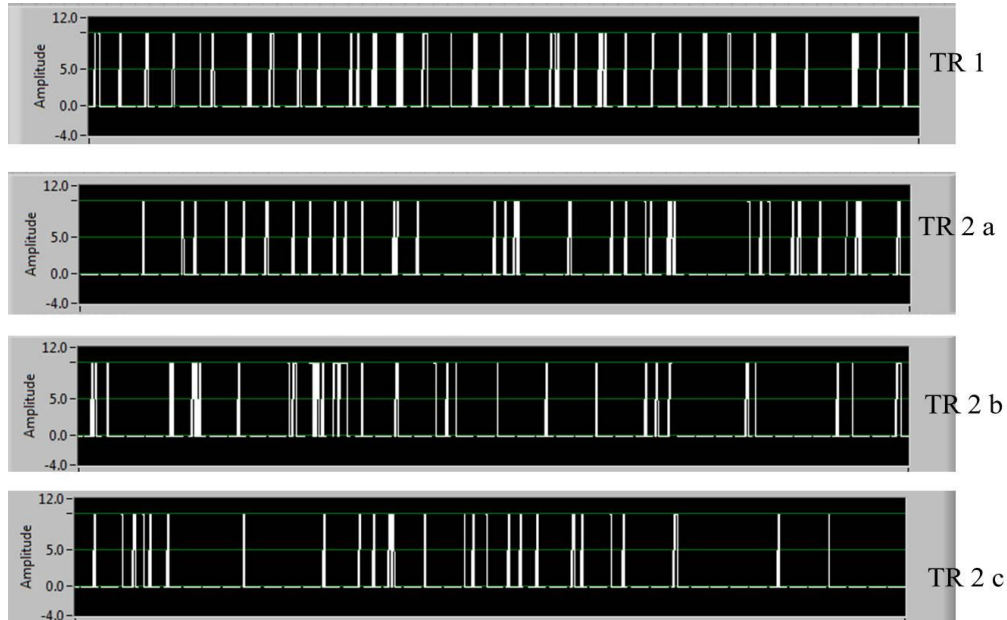


Figure 3. An example of the output of the transmitter-receivers used in the seed tubes with different curvature radiuses

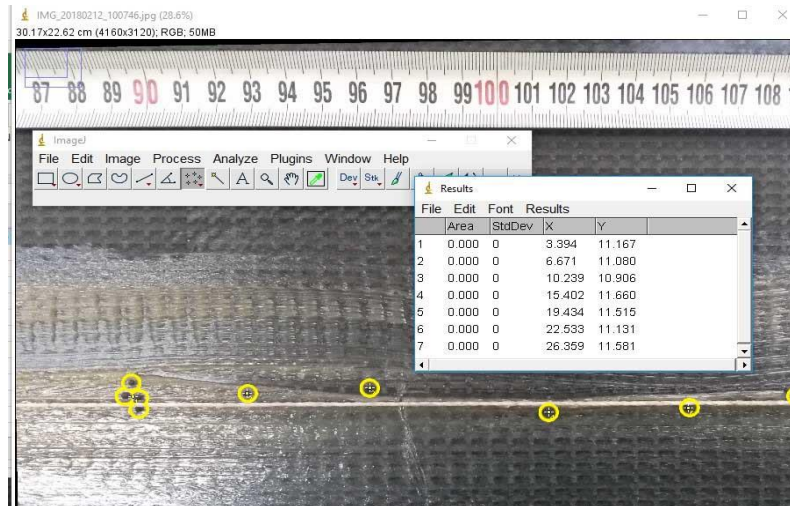


Figure 4. An example of images processed by ImageJ software to determine the location of the seeds distributed on the grease belt

## 2.2. Experimental conditions

The experiments were carried out at a travel speed of 0.5 m/s and air pressure of 490 Pa inside the seed tank. The distributor poured seeds on the grease belt in the cultivation row and then stopped for image acquisition. A ruler was put on the grease belt in parallel to the cultivation line, and the photos were then captured from the grease belt containing the seeds (Figure 4). Obtained images were analyzed using the ImageJ program, which is a conventional image processing software, and the distance of seeds from each other and from the cultivation line were measured. The uniformity coefficient of seed distribution in travel direction (x-axis) was calculated using Eq. (1) (Abdulkadir et al, 2019) for two modes: one based on the average distance of the seeds, and the other based on the adjusted distance of 2.5 cm

$$Se = 100 \times \left( 1 - \frac{Y}{D} \right) \quad (1)$$

where  $Se$  is the uniformity coefficient of seed distribution (%),  $D$  is the obtained or adjusted average distance between the seeds (mm), and  $Y$  is the meaning absolute of the difference from their average or adjusted distance (mm). The deviation of seeds' locations from the cultivation row in a perpendicular direction (y-axis) was also calculated in this study. All the experiments were conducted with five replications.

## 2.3. Response surface methodology for optimization

The effects of two independent variables, i.e., seed tube diameter and curvature radius, were investigated on the dependent variables, i.e., average distances in the x-axis and y-axis, using the Box-Behnken design. This method is based on a number of design points and a repeating center point. It is assumed that there are two mathematical functions  $f_k$  for  $Y_k$ , which considers the input arguments as natural units (Eq. 2) (Patt et al, 2020)

$$Y_k = f_k(\varepsilon_1, \varepsilon_2) \quad (2)$$

where  $\varepsilon_1$  and  $\varepsilon_2$  are the seed tube diameter and curvature radius, respectively. In RSM, the natural variables are converted to the coded variables (Eq. 3) (Patt et al, 2020)

$$Y_k = f_k(x_1, x_2) \quad (3)$$

In this study, a second-order polynomial model was used to model the process of seed distribution (Eq. 4) (Patt et al, 2020)

$$Y_k = \beta_0 + \sum_{i=1}^2 \beta_i x_i + \sum_{i=1}^2 \beta_{ii} x_i^2 + \sum_{i=1}^2 \sum_{j=i+1}^2 \beta_{ij} x_i x_j \quad (4)$$

**Table 1.** Independent variables and experiment design selective levels with results of each run

Run	Tube diameter (mm)	Tube curvature radius (cm)	Replication	X	Y
1	4.00	3.00	13.00	3.46	0.15
2	1.00	2.00	1.00	3.35	0.13
3	2.00	2.00	13.00	1.37	0.15
4	2.00	3.00	25.00	3.04	0.78
5	2.00	3.00	1.00	1.29	0.27
6	1.00	3.00	13.00	1.8	0.19
7	4.00	2.00	25.00	2.98	0.17
8	2.00	2.00	13.00	1.37	0.15
9	2.00	1.00	25.00	4.42	0.28
10	4.00	2.00	1.00	2.25	0.27
11	4.00	1.00	13.00	1.38	0.47
12	2.00	1.00	1.00	2.53	0.18
13	2.00	2.00	13.00	1.37	0.15
14	2.00	2.00	13.00	1.52	0.44
15	1.00	2.00	25.00	2.42	0.14
16	1.00	1.00	13.00	1.236	0.34
17	2.00	2.00	13.00	1.37	0.15

where  $Y_k$  ( $k=1,2$ ) is the predicted response and  $x_i$  ( $i=1,2$ ) is the encoded input variable. The value of independent variables was encoded within the range of -1 and +1.  $\beta$  values are regression coefficients. Using the second-order model, five mathematical models were assessed for each dependent variable. Therefore, 17 experimental units with five replications at the central point were obtained to determine the error value (Table 1). The significant terms in the model were obtained using the analysis of variance for each response.

**2.4. Prediction by partial least squares**

The PLS method is one of the most powerful techniques in factor analysis. The factors or principal components are a linear combination of the main variables in the matrices. It can change the variable space so that a linear combination of  $i$  factors produces new variables with the same information as previous variables (Malmir et al., 2020). Instead of finding a plan of maximum variances between responses and non-independent variables, the PLS method creates a relationship between the main components. Finally, a new regression model is created between the results of the input and output variables during a PLS modeling process. The model's performance is determined based on the coefficient of determination ( $R^2$ ) (Eq. 5)

$$R^2 = 1 - \frac{\sum_{i=1}^n (x_p - x_m)^2}{\sum_{i=1}^n (x_m - \bar{x}_m)^2} \tag{5}$$

where  $x_m$  is the measured value during the experiments,  $x_p$  is the predicted value, and  $n$  is the number of observations.

**Table 2.** Analysis of variance of the uniformity coefficient of seed distribution

Method	Independent variables	df	average of squares	F value
Adjusted average	Tube diameter	3	109.15	1.78 <sup>ns</sup>
	Tube curvature radius	2	35.67	0.58 <sup>ns</sup>
	Tube diameter × Tube curvature radius	6	29.30	0.48 <sup>ns</sup>
Obtained average	Tube diameter	3	202.32	0.90 <sup>ns</sup>
	Tube curvature radius	2	46.58	0.31 <sup>ns</sup>
	Tube diameter × Tube curvature radius	6	296.75	0.66 <sup>ns</sup>

ns: non-significant

**Table 3.** Analysis of variance of deviation from cultivation row

Independent variables	df	average of squares	F value
Tube diameter	3	0.50	12.58**
Tube curvature radius	2	0.47	11.87**
Tube diameter × Tube curvature radius	6	0.49	12.43**

\*\* Significant at 1% level

**2.5. Data analysis**

The analysis of variance was performed using SPSS v.26 (IBM, USA), while RSM was implemented in Design Expert (Stat-Ease Inc., USA). Additionally, the regression was performed using Unscrambler (CAMO AS, Trondheim, Norway).

**3. Results and Discussion**

**3.1. Results of uniformity analysis**

Due to the non-uniform airflow inside the seed tube, as well as the presence of curvature in the path of the seed tube, the separated seeds from the metering device passed from unequal paths. Therefore, the seed spacing on the cultivation row was not uniform despite the uniform separation from the distributor and placement in the seed tube. Table 2 shows the results of the analysis of variance of the uniformity coefficient of seed distribution considering the diameter and curvature radius of the seed tube. The uniformity coefficient was calculated once based on the adjusted average value and then based on the average value. According to the results, both the diameter and curvature radius of the seed tube did not have significant effects on the uniformity coefficients of the seeds in the travel direction. However, the effects of both variables and their interaction were significant ( $P < 0.01$ ) on the deviation of seed locations from the cultivation row (Table 4).

Table 5 shows the mean comparison of the uniformity coefficient based on the interaction of the seed tube parameters. The capital letters are used to compare the shapes at each diameter level, while small letters are utilized to compare the seed tube diameters at each shape level. According to the table, for the tube diameter of 5 mm, the deviation from the cultivation line was significantly higher for shape a than those of shapes b and c, with no significantly different values for shapes b and c.

**Table 4.** Results of mean comparison for the deviation from the cultivation line

Tube diameter (mm)	Tube curvature shape		
	a	b	c
5	0.27 <sup>Abc</sup>	0.14 <sup>Bc</sup>	0.15 <sup>Bc</sup>
7	0.19 <sup>Bc</sup>	0.24 <sup>Bb</sup>	0.30 <sup>Aa</sup>
9	0.28 <sup>Ab</sup>	0.32 <sup>Aa</sup>	0.21 <sup>Bb</sup>
11	0.43 <sup>Aa</sup>	0.22 <sup>Bb</sup>	0.25 <sup>Bb</sup>

For the tube diameter of 7 mm, shape c resulted in a higher deviation from the cultivation line than shapes a and b. In the tube diameter of 9 mm, the deviation from the cultivation line was the lowest for shape c. Finally, in the tube diameter of 11 mm, the deviation was significantly higher for shape a. For the shapes a to c, the diameters of 11, 9, and 7 mm, respectively, resulted in the highest deviation values. The diameters of 7, 5, and 5 mm exerted the lowest deviation for the shapes a to c, respectively. It can be concluded that the diameter of 5 mm had the lowest deviation from the cultivation line. However, due to the high variations for the seed tube shapes, it was impossible to introduce an appropriate shape with the lowest deviation values.

### 3.2. Results of the optimization

The values of independent variables were optimized to obtain the accurate distance between the seeds using RSM. Table 5 shows the results of the analysis of variance for the effect of the tube diameter and shape on seeds' distance in the x-axis (X). The optimization results were obtained using a quadratic model. The seed tube diameter and the seed tube curvature shape are specified with letters A and B, respectively. According to the results, the main and interaction effects of A and B treatments were significant on the X parameter ( $P < 0.05$ ). The  $R^2$  value of the model was 0.99, indicating the acceptable efficiency of the model in investigating the optimal points. A graphical representation of the effects of A and B treatments on X is depicted in Figure 5a. The lower X values indicate that the seeds are dispersed at a smaller distance from each other. The figure shows that by increasing the diameter of the seed tube to 7 mm and changing the shape of the seed tube to shape b, the seeds were dispersed on the belt with longer distances.

**Table 5.** Analysis of variance of RSM for the X parameter

Source	Sum (squares)	df	Mean (square)	F (Value)	Prob > F
Model	15.09859	11	1.258216	279.6036	< 0.0001
A	0.0729	1	0.0729	16.2	0.0158
B	1.7161	1	1.7161	381.3556	< 0.0001
A <sup>2</sup>	0.262106	1	0.262106	58.24585	0.0016
B <sup>2</sup>	0.429812	1	0.429812	95.51368	0.0006
AB	0.574564	1	0.574564	127.6809	0.0003
A <sup>2</sup> B	3.463712	1	3.463712	769.7138	< 0.0001
AB <sup>2</sup>	0.686792	1	0.686792	152.6204	0.0002
Pure Error	0.018	4	0.0045	-	-
Cor Total	15.11659	16	-	-	-

**Table 6.** Analysis of variance of RSM for the Y parameter

Source	Sum (squares)	df	Mean (square)	F (Value)	Prob > F
Model	0.397814	11	0.033151	1.970938	0.2685
A	0.007225	1	0.007225	0.429548	0.5480
B	0.087025	1	0.087025	5.1739	0.0853
A <sup>2</sup>	0.015284	1	0.015284	0.908708	0.3944
B <sup>2</sup>	0.082232	1	0.082232	4.888932	0.0915
AB	0.007225	1	0.007225	0.429548	0.5480
BC	0.042025	1	0.042025	2.498514	0.1891
A <sup>2</sup> B	0.14045	1	0.14045	8.350178	0.0446
AB <sup>2</sup>	0.0008	1	0.0008	0.047562	0.8380
Pure Error	0.06728	4	0.01682	-	-
Cor Total	0.465094	16	-	-	-

**Table 7.** Regression model of the response surface methodology

Parameter	Mean	R <sup>2</sup>	Equation
X	2.19	0.99	$X = +1.40 - 0.14 \times A - 0.65 \times B + 0.25 \times A^2 + 0.32 \times B^2 + 0.38 \times AB + 1.32 \times A^2B + 0.59 \times AB^2$
Y	0.26	0.85	$Y = +0.21 + 0.043 \times A + 0.15 \times B - 0.060 \times A^2 + 0.14 \times B^2 - 0.042 \times AB - 0.27 \times A^2B - 0.020 \times AB^2$

**Table 8.** The solutions founded by RSM during the optimization

Number	Tube diameter	Tube curvature radius	X	Y	Desirability
1	1.00	1.00	1.20933	0.00	1
2	1.00	1.00	1.21636	0.00	1
3	1.00	1.00	1.2251	0.00	0.999999
4	1.00	1.00	1.23449	0.00	0.999999
5	1.00	1.00	1.24904	0.00	0.997949
6	1.00	1.77	1.66648	0.00	0.929944
7	2.00	3.00	1.43426	0.00	0.92384
8	1.00	3.00	1.41013	0.00	0.923782

The results of the analysis of variance for the seeds' distance in the y-axis (Y) are represented in Table 6. Both A and B treatments showed no significant effects on the Y parameter. Meanwhile, only the effects of A<sup>2</sup>B (i.e., the product of the squared value of seed tube diameter and tube shape) were significant ( $P < 0.05$ ). The changes in the Y parameter are shown in Figure 5b as a function of the seed tube diameter and shape. As shown in the figure, Y increased by increasing the seed tube diameter. Moreover, the shape of the seed tube caused a change in Y. It can be said that the optimal point can be obtained at the diameter of 8 mm and the tube shape b.

The effects of the seed tube diameter and shape parameters were investigated according to the results of RSM (Table 7) as a quadratic regression model. The sign (+) indicates the positive effect, while the sign (-) indicates the negative effect. The mean value of X was 2.19 mm, which could be modeled by the quadratic regression model with an  $R^2$  of 0.99. According to the equations, X decreased by increasing A and B. By increasing A<sup>2</sup> and B<sup>2</sup>, X increased, and the interaction effects of A and B caused an increase in X. Moreover, Y was modeled with an  $R^2$  of 0.85. Y increased by increasing A and B. Moreover, A<sup>2</sup> and B<sup>2</sup> were inversely and directly related to Y, respectively. Finally, all AB, A<sup>2</sup>B, and AB<sup>2</sup> were inversely related to Y.

Table 8 shows the RSM results to find the best optimal points. The desirability index is the index confirming the model in the optimization of parameters. According to the results, all the suggested models have the best desirability index, indicating that the optimal values of X and Y will be obtained, and the desirability index will be at its highest level if the diameter and shape of the seed tube have the values suggested in the table.

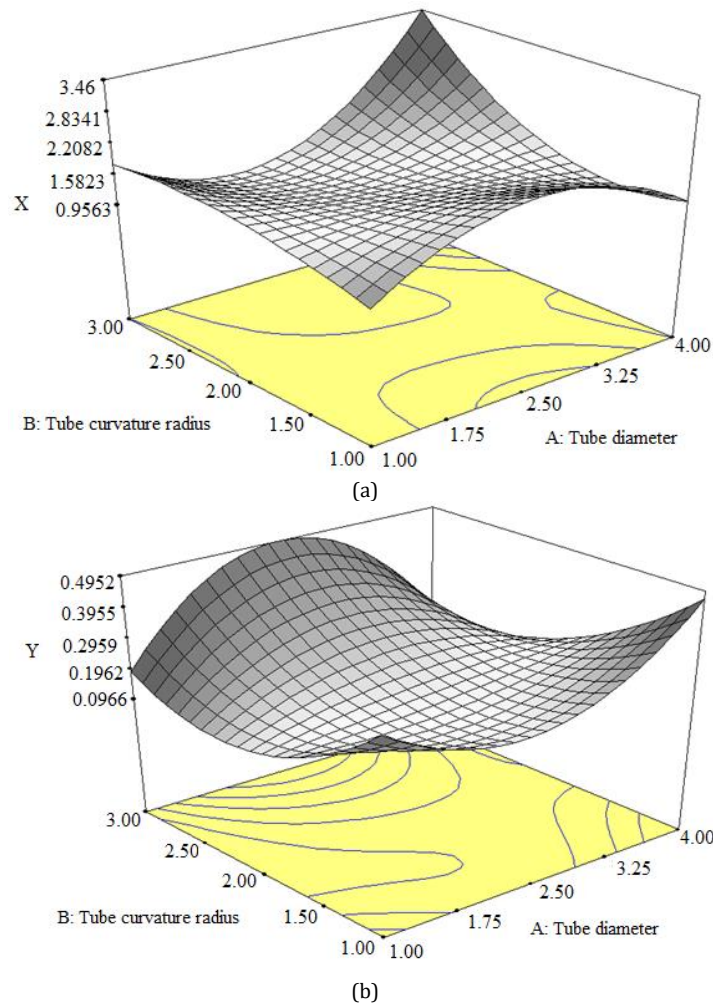


Figure 5. Results of RSM in optimizing the average distance of seeds in (a) travel direction, (b) perpendicular direction

**3.3. Results of prediction using partial least squares**

PLS was used in this study to predict the seeds’ distance having the values of the diameter and curvature radius of the seed tube. Figure 6 shows the predicted values versus the real data obtained during the experiments. The results showed that the PLS method could predict the data of seeds’ locations on the grease belt with an  $R^2$  of 99%.

**4. Conclusion**

One of the most important issues in agriculture is planting seeds in agricultural farms by planters. Most practical planters

are of the linear type, and the seeds are planted linearly in the ground. In this research, an online image processing system is used to investigate the exact distance between seeds in a laboratory setup. A distributor with a seed tube of different diameters and shapes was used during the experiments. The experimental data were optimized by RSM to obtain the most accurate distance between the distributed seeds, and the data were predicted by the PLS method. The findings of this study are useful when designing new generations of pneumatic seed planters with optimized seed tubes to obtain the best planting results

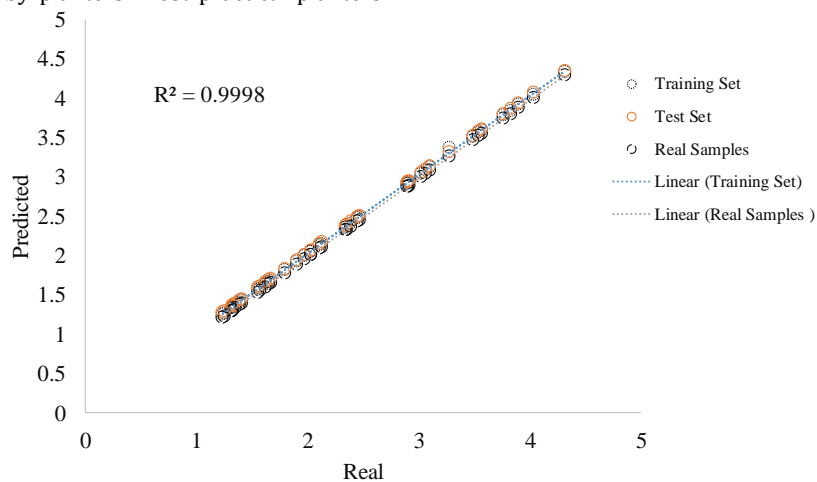


Figure 6. Prediction of the observation data of the average distance of the seeds having the diameter and curvature radius of the seed tube

## References

- Abdulkadir, T. D., Mahadi, M. R., Wayayok, A., & Kassim, M. S. M. (2019). Operational parameters affecting pneumatic paddy seeds handling using vacuum pressure. *Agricultural Engineering International: CIGR Journal*, 21(2).
- An, X., Wang, S., Duan, H., Yang, C., & Yu, Y. (2017). Test on effect of the operating speed of maize-soybean interplanting seeders on performance of seeder-metering devices. *Procedia Engineering*, 174, 353–359. <https://doi.org/10.1016/j.proeng.2017.01.153>
- Asefpour Vakilian, K. & Massah, J. (2017). A farmer-assistant robot for nitrogen fertilizing management of greenhouse crops. *Computers and Electronics in Agriculture*, 139, 153–163. <https://doi.org/10.1016/j.compag.2017.05.012>
- Barth, R., Hemming, J., & Van Henten, E. J. (2019). Angle estimation between plant parts for grasp optimisation in harvest robots. *Biosystems Engineering*, 183, 26–46. <https://doi.org/10.1016/j.biosystemseng.2019.04.006>
- Cay, A., Kocabiyik, H., & May, S. (2018a). Development of an electro-mechanic control system for seed-metering unit of single seed corn planters Part I: Design and laboratory simulation. *Computers and Electronics in Agriculture*, 144, 71–79. <https://doi.org/10.1016/j.compag.2017.11.035>
- Cay, A., Kocabiyik, H., and May, S., 2018b. Development of an electro-mechanic control system for seed-metering unit of single seed corn planters Part II: Design and laboratory simulation. *Computers and Electronics in Agriculture*, 144, 11–17. <https://doi.org/10.1016/j.compag.2017.11.035>
- Deng, X., Li, X., Shu, C., Huang, H., Liao, Q., XiaoYan, D., Xu, L., CaiXia, S., HaiDong, H., & QingXi, L. (2010). Mathematical model and optimization of structure and operating parameters of pneumatic precision metering device for rapeseed. *Journal of Food, Agriculture and Environment*, 8, 318–322.
- Dubey, S. R. & Jalal, A. S. (2015). Application of image processing in fruit and vegetable analysis: A review. *Journal of Intelligent Systems*, 24(4), 405–424. <https://doi.org/10.1515/jisys-2014-0079>
- Fellegari, R., & Navid, H. (2011). Determining the orange volume using image processing. In *International Conference on Food Engineering and Biotechnology (ICFEB 2011)* (pp. 180–184).
- Garg, A., Shrivastava, C., Murai, Y., & Windhab, E. J. (2019). Impact of airflow on the heat transfer conditions inside an oven cavity, characterized using particle imaging velocimetry. *Physics of Fluids*, 31(10), 107109. <https://doi.org/10.1063/1.5122800>
- Guarella, P., Pellerano, A., & Pascuzzi, S. (1996). Experimental and theoretical performance of a vacuum seeder nozzle for vegetable seeds. *Journal of Agricultural Engineering Research*, 64, 29–36. <https://doi.org/10.1006/jaer.1996.0043>
- Iacomi, C., & Popescu, O. (2015). A New Concept for seed precision planting. *Agriculture and Agricultural Science Procedia*, 6, 38–43. <https://doi.org/10.1016/j.aaspro.2015.08.035>
- Ibrahim, E. J., Liao, Q., Wang, L., Liao, Y., & Yao, L. (2018). Design and experiment of multi-row pneumatic precision metering device for rapeseed. *International Journal of Agricultural and Biological Engineering*, 11(5), 116–123. <https://doi.org/10.25165/j.ijabe.20181105.3544>
- Karayel, D. (2009). Performance of a modified precision vacuum seeder for no-till sowing of maize and soybean. *Soil and Tillage Research*, 104, 121–125. <https://doi.org/10.1016/j.still.2009.02.001>
- Karayel, D., Barut, Z. B., & Özmerzi, A. (2004). Mathematical modelling of vacuum pressure on a precision seeder. *Biosystems Engineering*, 87, 437–444. <https://doi.org/10.1016/j.biosystemseng.2004.01.011>
- Ma, H., Shen, S., Yu, M., Yang, Z., Fei, M., & Zhou, H. (2019). Multi-population techniques in nature inspired optimization algorithms: A comprehensive survey. *Swarm and Evolutionary Computation*, 44, 365–387. <https://doi.org/10.1016/j.swevo.2018.04.011>
- Maleki, M. R., Jafari, J. F., Raufat, M. H., Mouazen, A. M., & Baerdemaeker, J. (2006). Evaluation of seed distribution uniformity of a multi-flight auger as a grain drill metering device. *Biosystems Engineering*, 94, 535–543. <https://doi.org/10.1016/j.biosystemseng.2006.04.003>
- Malmir, M., Tahmasbian, I., Xu, Z., Farrar, M. B., & Bai, S. H. (2020). Prediction of macronutrients in plant leaves using chemometric analysis and wavelength selection. *Journal of Soils and Sediments*, 20(1), 249–259. <https://doi.org/10.1007/s11368-019-02418-z>
- Meruliya, T., Dhameiliya, P., Patel, J., Panchal, D., Kadam, P., & Naik, S., (2015). Image processing for fruit shape and texture feature extraction-review. *International Journal of Computer Applications*, 975, 30–33.
- Morimoto, T., Takeuchi, T., Miyata, H., & Hashimoto, Y. (2000). Pattern recognition of fruit shape based on the concept of chaos and neural networks. *Computers and Electronics in Agriculture*, 26(2), 171–186. [https://doi.org/10.1016/S0168-1699\(00\)00070-3](https://doi.org/10.1016/S0168-1699(00)00070-3)
- Önal, İ., Değirmenciöglü, A., & Yazgi, A. (2012). An evaluation of seed spacing accuracy of a vacuum type precision metering unit based on theoretical considerations and experiment. *Turkish Journal of Agriculture and Forestry*, 36, 133–144. <https://doi.org/10.3906/tar-1010-1316>
- Özmerzi, A., Karayel, D., & Topakci, M. (2002). Effect of sowing depth on precision seeder uniformity. *Biosystems Engineering*, 82, 227–230. <https://doi.org/10.1006/bioe.2002.0057>
- Patt, J. M., Tarshis Moreno, A. M., & Niedz, R. P. (2020). Response surface methodology reveals proportionality effects of plant species in conservation plantings on occurrence of generalist predatory arthropods. *PLoS one*, 15(4), e0231471. <https://doi.org/10.1371/journal.pone.0231471>
- Popa, C. V., Vasilescu, A., Litescu, S. C., Albu, C., & Danet, A. F. (2020). Metal nano-oxide based colorimetric sensor array for the determination of plant polyphenols with antioxidant properties. *Analytical Letters*, 53(4), 627–645. <https://doi.org/10.1080/00032719.2019.1662430>
- Sarlaki, E., Sharif Paghaleh, A., Kianmehr, M.H., & Asefpour Vakilian, K., (2020). Valorization of lignite waste into humic acids: Process optimization, energy efficiency and structural features analysis. *Renewable Energy*, 163, 105–122. <https://doi.org/10.1016/j.renene.2020.08.096>
- Scheidt, W., dos Santos Pedroza, I. C. P., Fontana, J., da Cruz Meleiro, L. A., de Barros Soares, L. H., & Reis, V. M. (2020). Optimization of culture medium and growth conditions of the plant growth-promoting bacterium *Herbaspirillum seropedicae* BR11417 for its use as an agricultural inoculant using response surface methodology (RSM). *Plant and Soil*, 451(1), 75–87. <https://doi.org/10.1007/s11104-019-04172-0>
- Singh, R. C., Singh, G., & Saraswat, D. C. (2005). Optimisation of design and operational parameters of a pneumatic seed metering device for planting cottonseeds. *Biosystems Engineering*, 92, 429–438. <https://doi.org/10.1016/j.biosystemseng.2005.07.002>
- Tang, J. L., Chen, X. Q., Miao, R. H., & Wang, D. (2016). Weed detection using image processing under different illumination for site-specific areas spraying. *Computers and Electronics in Agriculture*, 122, 103–111. <https://doi.org/10.1016/j.compag.2015.12.016>
- Wang, A., Zhang, W., & Wei, X. (2019). A review on weed detection using ground-based machine vision and image processing techniques. *Computers and Electronics in Agriculture*, 158, 226–240. <https://doi.org/10.1016/j.compag.2019.02.005>
- Yasir, S.H., Liao, Q., Yu, J., & He, D. (2012). Design and test of a pneumatic precision metering device for wheat. *Agricultural Engineering International: CIGR Journal*, 14, 16–25.
- Yazgi, A. & Degirmencioglu, A. (2007). Optimisation of the seed spacing uniformity performance of a vacuum-type precision seeder using response surface methodology. *Biosystems Engineering*, 97, 347–356. <https://doi.org/10.1016/j.biosystemseng.2007.03.013>
- Yazgi, A. & Degirmencioglu, A. (2014). Measurement of seed spacing uniformity performance of a precision metering unit as function of the number of holes on vacuum plate. *Measurement*, 56, 128–135. <https://doi.org/10.1016/j.measurement.2014.06.026>
- Zhai, Z., Zhu, Z., Du, Y., Song, Z., & Mao, E. (2016). Multi-crop-row detection algorithm based on binocular vision. *Biosystems Engineering*, 150, 89–103. <https://doi.org/10.1016/j.biosystemseng.2016.07.009>
- Zhan, Z., Yaoming, L., Jin, C., & Lizhang, X. (2010). Numerical analysis and laboratory testing of seed spacing uniformity performance for vacuum-cylinder precision seeder. *Biosystems Engineering*, 106, 344–351. <https://doi.org/10.1016/j.biosystemseng.2010.02.012>
- Zhang, S., You, Z., & Wu, X. (2019). Plant disease leaf image segmentation based on superpixel clustering and EM algorithm. *Neural Computing and Applications*, 31(2), 1225–1232. <https://doi.org/10.1007/s00521-017-3067-8>